

direction might produce a $\mathbf{V} \times \mathbf{E}$ effect that would be influenced by stray magnetic fields of neighboring equipment. After the conclusion of the experiment, tests were made with a search coil to measure the vertical component of the magnetic field within the magnet. There did appear to be a change over a period of several weeks which would change the orientation of the magnetic field with respect to the pole faces by a few milliradians.

Since the fluctuations in the value of μ_e as evaluated in each run cannot be explained on the basis of counting statistics, we feel that exact limits cannot be specified for an upper limit to a possible electric dipole moment.

One can say, however, that these results are consistent with those of Shull and Nathans⁷ [$(+2.4 \pm 3.9) \times 10^{-22}$ e cm] diffraction experiment and Dress *et al.*⁵ ($|\mu_e| < 3 \times 10^{-22}$ e cm) and not consistent with theoretical predictions appreciably greater than 10^{-21} e cm.⁶

We are greatly indebted to James Fenton and Anthony Meade for assistance in the apparatus design; John Ciperano and Alfred W. Kane for technical assistance both in the assembly and operation of equipment, and Robert Chase and Martin Rosenblum of the Instrumentation Department for development of some of the critical components of the data-processing equipment.

Search for (Σ^-n) and (Σ^-nn) Bound States*

R. A. BURNSTEIN, W. C. CUMMINGS, D. L. SWANSON, AND V. R. VEIRS

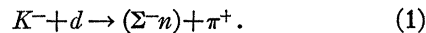
Illinois Institute of Technology, Chicago, Illinois 60616

(Received 16 May, 1968)

In an experiment involving K^- capture in helium, a search was made for (Σ^-n) and (Σ^-nn) bound states as produced by the following reactions: $K^- + \text{He}^4 \rightarrow (\Sigma^-n) + \pi^+ + d$; $K^- + \text{He}^4 \rightarrow (\Sigma^-nn) + \pi^+ + p$. We did not find any unambiguous examples of these reactions among the interactions of 8370 stopping K^- mesons. Upper limits on the rates for the production of these bound hyperon states are determined, relative to various K^- capture reactions. With respect to stopping K^- mesons, an upper limit on the bound-state production rate is $\leq 0.02\%$, using one ambiguous bound-state event for calculational purposes. In addition, for these data, we do not find evidence for a maximally strong (Σ^-n) final-state interaction.

I. INTRODUCTION

PREVIOUSLY, there have been a number of searches for bound states of hyperons in nuclear emulsions with inconclusive results.¹⁻³ A bubble-chamber experiment, involving K^- -deuterium capture at rest,⁴ searched for the (Σ^-n) bound state as produced by the two-body reaction



By angular momentum and parity-conservation selection rules, only the triplet state can be produced. The result of this experiment was to set a limit of $\lesssim 1\%$ to the fraction of Σ^- hyperons forming a triplet (Σ^-n) bound state. This deuterium capture experiment could not detect a singlet (Σ^-n) bound state.

Recent experiments on Σ -proton scattering indicate a weak triplet Σ -nucleon interaction.⁵ So if there is a Σ -nucleon bound state, it could be expected to occur as a singlet (Σ^-n) bound state. In helium, in contrast to deuterium, there are no selection rule restrictions, since there is a three-body final state, and, therefore, K^- capture can produce a singlet (Σ^-n) bound state.⁶ In this paper, we report on a search for the (Σ^-n) and the (Σ^-nn) bound states from K^- capture in helium.

II. EXPERIMENTAL PROCEDURE

A two-stage, electrostatically separated beam was designed and built at the Argonne zero-gradient synchrotron (ZGS) to provide 600–850 MeV/c K^- mesons. The details and parameters of the beam are described elsewhere.⁷ In this experiment the K^- beam was transported at 650 MeV/c, then slowed down by a moderator and the copper surrounding the Argonne National

* Work supported in part by the Research Corporation and the National Science Foundation.

¹ M. Baldo-Ceolin, W. F. Fry, W. D. B. Greening, H. Huzita, and S. Limentani, *Nuovo Cimento* **6**, 144 (1957).

² E. Gandolfi, J. Heughebaert, and E. Quercigh, *Nuovo Cimento* **13**, 864 (1959).

³ R. G. Ammar, N. Crayton, K. P. Jain, R. Levi Setti, J. E. Mott, P. E. Schlein, O. Skjeggstad, and P. K. Srivastava, *Phys. Rev.* **120**, 1914 (1960).

⁴ O. Dahl, N. Horwitz, D. Miller, and J. Murray, *Phys. Rev. Letters* **4**, 428 (1960).

⁵ H. G. Dosch, R. Englemann, H. Filthuth, V. Hepp, and E. Kluge, *Phys. Letters* **21**, 236 (1966); and H. A. Rubin and R. A. Burnstein, *Phys. Rev.* **159**, 1149 (1967).

⁶ For a discussion indicating that many partial waves are involved in a K^- capture reaction with a three-body final state, see R. Karplus and L. Rodberg, *Phys. Rev.* **115**, 1058 (1959).

⁷ M. Derrick and G. Keyes, in *Proceedings of the 1966 International Conference on Instrumentation for High-Energy Physics* (North-Holland Publishing Company, Amsterdam, 1967), p. 618.

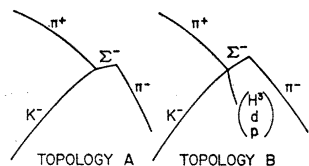
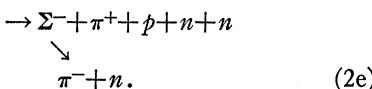
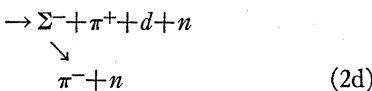
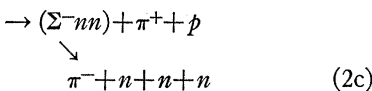
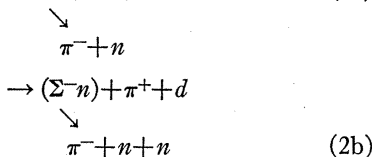
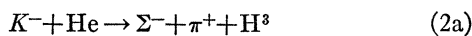


FIG. 1. Line drawing of topologies searched for in the scanning of the bubble-chamber film. Topology *A* involves an incident K^- , an outgoing π^+ , and an outgoing particle which decays. Topology *B* is similar except that there is an additional visible heavily ionizing track (prong) at the production vertex.

Laboratory-Carnegie 25-cm liquid-helium bubble chamber.^{8,9} The momentum of the beam as it entered the bubble chamber was $\sim 200 \pm 30$ MeV/c.¹⁰ About one stopping and one in-flight K^- meson appeared in the chamber per pulse. The magnetic field was produced by a superconducting magnet with a central field of ~ 40.5 kG.⁹ The field variation was $\sim \pm 10\%$ over the useful volume of the chamber.

The hyperon production and decay reactions which are the basis of this study are the following:



All the production and decay reactions have two similar topologies: topology *A* and topology *B*, which are shown in Fig. 1. These topologies differ in whether there is a visible nucleon track at the production vertex. The first topology (*A*, Fig. 1) involves an incident K^- , an outgoing π^+ , and an outgoing particle which decays. The second topology (*B*, Fig. 1) is identical except that there is an additional visible heavily ionizing outgoing track which represents either a triton, a deuteron, or a proton. The events are recorded by the scanners and measured according to which topology they represent. If the nucleon track is very short and not visible in at least two of the three views, then topology *B* becomes topology *A* for measurement purposes. We found 720

⁸ M. Derrick, Ref. 7, p. 431.

⁹ M. Derrick, T. H. Fields, L. Hyman, J. Loken, K. Martin, E. G. Pewitt, J. Fetkovitch, and J. McKenzie, Ref. 7, p. 264; C. Laverick and G. M. Lobell, Rev. Sci. Instr. **36**, 825 (1965).

¹⁰ J. H. Boyd, R. A. Burnstein, J. G. McComas, and V. R. Veirs, Phys. Rev. Letters **19**, 1405 (1967).

examples¹¹ of topology *A* or *B* in a study involving 12 500 frames of film, containing ~ 8370 stopping K^- mesons. This sample of film was double scanned with an over-all efficiency of $(95 \pm 3)\%$.

III. RESULTS

A process basic to this experiment is the procedure whereby an event is associated with a specific production reaction (2a)-(2e). The track measurements are converted into space coordinates by the program TVGP¹² and then kinematically fitted by the program SQUAW¹³ to the hypotheses of the various hyperon production and decay reactions. Events which are inconsistent with the hypothesis of a K^- interaction at rest are not considered further. This restriction is made since a K^- interaction at rest has a very well determined K^- momentum ($p_{K^-} = 0.0$ MeV/c) and this results in improved resolution for tests of the various production hypotheses. The separation between at-rest and in-flight interactions is accomplished by requiring that the measured unfit K^- momentum be ≤ 115 MeV/c for events where the K^- momentum is well determined ($l_{K^-} \geq 5$ cm, $\Delta p/p \lesssim 0.2$). The unfitted K^- momentum has to be used since reaction (2e) cannot be fitted and we need an additional criterion which is independent of the reaction under consideration. The feasibility of using unfitted momenta so close to the stopping region depends on the superior momentum resolution and accurate calibration of the bubble chamber.¹⁴ As a check, plots [Figs. 2(a) and 2(b)] of the distribution of unfit measured momenta and residual ranges of 450 randomly selected slow K^- were symmetric and contained no events "overstopped" by more than 115 MeV/c. For this reason the requirement $p_{K^-} \leq 115$ MeV/c separates out the sample of stopping K^- interactions. In the stopping sample, there are a negligible number of in-flight interactions with $p_{K^-} \leq 115$ MeV/c, since the pathlength is small for this interval.

The measured events fall into two categories, topology *A* and topology *B*. For those events in topology *B*, the category with a nucleon track at the production vertex, there are constrained fits¹⁵ to the following reactions: (2a), (2b), (2c), and (2d). Reaction (2e), $K^- + \text{He}^4 \rightarrow \Sigma^- + \pi^+ + p + n + n$, involves too many missing neutral particles to be fitted. The number of Σ^- produced in this channel (2e) for topology *B* is determined by subtracting the number of examples of reactions (2a) and (2d) (in topology *B*) from the total number of Σ^-

¹¹ This number includes events which were subsequently rejected by the cuts or suffered measurement failures.

¹² D. Johnson, F. T. Solmitz, and T. B. Day, Lawrence Radiation Laboratory Programmer's Note P-117, 1965 (unpublished).

¹³ O. I. Dahl, T. B. Day, and F. T. Solmitz, Lawrence Radiation Laboratory Programmer's Note P-126, 1965 (unpublished).

¹⁴ L. G. Hyman, J. Loken, E. G. Pewitt, M. Derrick, T. Fields, J. McKenzie, I. Wang, J. Fetkovitch, and G. Keyes, Phys. Letters **25B**, 376 (1967).

¹⁵ It is to be noted that the distribution of observed χ^2 in this experiment [for reaction (2a)] agrees well with theoretical expectations.

hyperons produced with visible nucleons from stopping K^- . For topology *A*, events with no visible nucleon track at the production vertex, there is a 1-constraint fit for one reaction (2a).¹⁶ For the other reactions in topology *A*, (2d) and (2e) which cannot be fitted, it is possible to estimate the number of events of the type involving an invisible nucleon. The number of events with invisible nucleons (topology *A*), is deduced by comparing the observed spectra with phase-space predictions. The total number of events in a given channel is the sum of the number of events in topology *A* and topology *B* for that channel. This is the basis for our determination of the number of events in the various Σ^- production channels. These results will be applied to our determination of the rates for (Σ^-n) and (Σ^-nn) bound state production.

The identification of (Σ^-n) and (Σ^-nn) bound-state production events from among ordinary Σ^- production was carried out in the following manner. This task is separated into two aspects. The first is a search for unambiguous (Σ^-n) and (Σ^-nn) bound-state events, and the second is a search for possible (Σ^-n) and (Σ^-nn) bound states.

The criterion for an unambiguous Σ^- -nucleon bound-state event is that it fit the hypothesis¹⁵ of (2b) or (2c) with a confidence level $P(\chi^2) \geq 0.1\%$ but not hypotheses (2a) or (2d) with a confidence level $P(\chi^2) \geq 1\%$. An important result of this experiment is that we have not found any events which satisfy this criterion, which implies that we do not find any evidence for unambiguous (Σ^-n) or (Σ^-nn) bound-state production.

The criterion for a possible Σ^- -nucleon bound-state event is that it fit the hypothesis¹⁵ of (2b) or (2c) with a confidence level $P(\chi^2) \geq 0.1\%$ but also simultaneously be consistent with reaction (2a) or (2d) with a confidence level $P(\chi^2) \geq 1\%$. In this way we have found one event which is either a possible (Σ^-n) bound-state event or this same event is a possible (Σ^-nn) bound-state event. The confidence levels for the fits and other information is shown in Table I, for this one possible bound-state event. It is to be noted for this one event that the confidence levels are also high for the hypotheses of reaction (2a) and (2d)—ordinary events.¹⁷

The classification of an event as an unambiguous or a possible (Σ^-n) and (Σ^-nn) bound state has not involved

¹⁶ An additional constraint is obtained when the Σ^- momentum can be determined from track curvatures. This is possible for $l_{\Sigma^-} > 1$ cm, because of the high magnetic field. The number of these cases is sufficiently small so that it has not been necessary to alter the analysis procedure described.

¹⁷ The explanation has been advanced that the event in Table I is an example of an ordinary Σ^- production reaction which accidentally fits the (Σ^-nn) bound-state hypothesis. On the other hand, the converse could apply—that the event is truly a (Σ^-n) bound-state event which accidentally fits the ordinary Σ^- production reactions. It is not likely that a (Σ^-n) bound-state event (3-constraint) will fit the hypothesis of the reaction $\Sigma^- + \pi^+ + H^0$ and subsequent Σ^- decay. This sequence involves more constraints (4-constraint), since there is the additional requirement of fitting the Σ^- decay, and one does not expect accidental fits involving a higher constraint class.

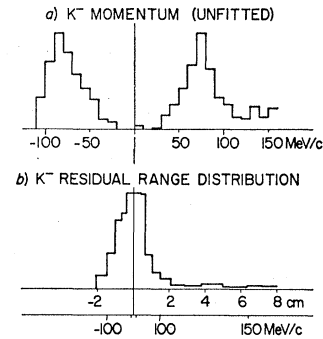


FIG. 2. (a) Plot of the distribution of unfitted measured momenta of randomly selected slow K^- beam tracks. The events to the left of zero, $p_{K^-} \leq 0$, are called "overstopped" K^- and the events to the right of zero, $p_{K^-} \geq 0$, are called "understopped" K^- . Events with $p_{K^-} \geq +115$ MeV/c are in-flight K^- . The stopping K^- are contained in the interval $p_{K^-} \leq 115$ MeV/c. (b) Plot of the residual range distribution for the same sample of randomly selected slow K^- beam tracks as used for (a).

any criterion concerning the projected length of the nucleon track. It would be reasonable to impose this criterion since the projected length of the nucleon track should be greater than ~ 1 mm in order to constrain the fit; 1 mm is the order of several bubbles. If this 1-mm cut were applied to our data, then the one possible bound-state event would be eliminated by this requirement. This cut would result in a small loss of events, $\sim 7\%$, in the total number of examples of topology *B*. We have not incorporated this criterion into our analysis because such a consideration is somewhat arbitrary and the process is *ad hoc*.

IV. DISCUSSION

From Sec. III we concluded that we did not find any unambiguous examples of (Σ^-n) and (Σ^-nn) bound-state production. However, we concluded that there was one event which was either a possible (Σ^-n) bound-state event or a possible (Σ^-nn) bound-state event. These observations can be converted into upper limits on the rate for the production of Σ^- -nucleon bound states with reference to various K^- capture reactions.

The numerator for the (Σ^-n) production rate is the number of observed production events which is taken to be one for calculational purposes. A more accurate estimate of the numerator can be obtained if the observed number of production events (one) is scaled up by a factor to take into account the fact that the entire production spectrum cannot be observed. This is a

TABLE I. Possible Σ^- -nucleon bound-state event.*

Frame number	$P(\chi^2)$ (Σ^-n)	$P(\chi^2)$ (Σ^-nn)	$P(\chi^2)$ $\Sigma^- + \pi^+ + H^0$	$P(\chi^2)$ $\Sigma^- + \pi^+ + d + n$	Projected length of nucleon track
173 208	55%	17%	98%	63%	0.5 mm

* The values in the table are based on six measurements of the event. Each of the six measurements is consistent with the average value.

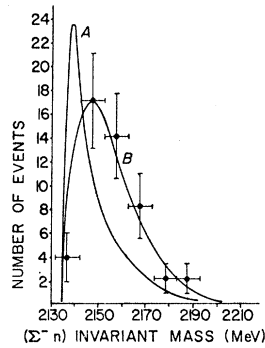


FIG. 3. Plot of invariant mass of the (Σ^-n) system from events produced in the reaction $K^- + \text{He}^4 \rightarrow \Sigma^- + \pi^+ + d + n$ with visible deuterons. Curve A assumes a maximally strong final-state interaction, as discussed in Ref. 21, and does not agree with the data $P(\chi^2) \approx 10^{-6}$. Curve B assumes a weaker final-state interaction and agrees with the data $P(\chi^2) \approx 0.47$.

consequence of the fact that deuteron projected lengths which are $\lesssim 1$ mm are not always visible. The calculation of the exact number of deuterons (events) which cannot be observed depends on the (Σ^-n) production model chosen. One possible mechanism for the production of a (Σ^-n) bound state involves a two-step process in helium. This model assumes an impulse picture (Appendix describes this type of calculation) for K^- capture in He^4 and as the first step, $K^- + p \rightarrow \Sigma^- + \pi^+$ with $(d+n)$ as spectators. The second step involves production of (Σ^-n) due to a strong final-state interaction between the Σ^- and n in the reaction $\Sigma^- + \pi^+ + d + n$. We assume that the deuteron energy spectrum for the (Σ^-n) bound-state events is similar to the $(d+n)$ energy spectrum since it is more likely that low-energy neutrons form bound (Σ^-n) systems. Thus, the deuteron energy spectrum should not be altered significantly from the $(d+n)$ energy spectrum. The results of this calculation lead to the result that the portion of the spectrum observable in this experiment for deuterons whose projected length is ≥ 1 mm is $\sim 70\%$. Another possible mechanism for the production of a (Σ^-n) bound state is via the one-step process $K^- + \text{He} \rightarrow (\Sigma^-n) + \pi^+ + d$, where K^- interacts with two nucleons simultaneously, a common phenomenon in helium ($\sim 18\%$ ¹⁸). Appendix A gives the details of this impulse-model calculation. Figure 5 shows the predicted momentum spectrum from which we derive the result that the portion of the spectrum observable in this experiment for deuterons whose projected length is ≥ 1 mm is 65% . For both the models discussed, the results are similar, thus indicating that the conclusions are not sensitive to the type of impulse model assumed. On the other hand, if a phase-space calculation were used, $\sim 90\%$ of the deuteron spectrum would be observable. In order to set an *upper limit* for the total number of (Σ^-n) bound states produced, we have used the results of the one-step bound-state production model.

The numerator of the (Σ^-nn) production rate is the number of observed production events. The number of

such events has been given the value of one event for calculational purposes. Estimates similar to the ones described previously, for the portion of the production spectrum which cannot be observed, have been obtained by using impulse-model calculations assuming that the (Σ^-nn) bound state is either produced by a two-step process or by a one-step process. In this way, we obtain the estimate that the portion of the proton spectrum observable in this experiment [associated with the reaction $(\Sigma^-nn) + \pi^+ + p$], whose projected length is greater than 1 mm is $\sim 95\%$ (two step) and 90% (one step). In order to set an *upper limit* for the total number of (Σ^-nn) bound states produced, we have used the results of the one-step bound-state production model.

The denominator, in the calculation of the (Σ^-n) and the (Σ^-nn) production rates is the total number of events in the specific channels considered.¹⁹ A summary of our rate determinations is shown in Table II.²⁰ Reaction (2d), $\Sigma^- + \pi^+ + d + n$ in topologies A and B, occurs $(12 \pm 4.5)\%$ of the time relative to the production of all Σ^- hyperons (with π^+). The rate of (Σ^-n) bound-state production relative to this reaction (2d) is $\leq 3.0\%$. Reaction (2e), $\Sigma^- + \pi^+ + p + n + n$ in topologies A and B, occurs $(29 \pm 4)\%$ of the time. The rate of (Σ^-n) bound-state production relative to this reaction is $\leq 1.0\%$, and the corresponding (Σ^-nn) bound-state production rate is $\leq 0.7\%$. Finally, the rates of (Σ^-n) and (Σ^-nn) bound-state events relative to all events where Σ^- hyperons are produced (with π^+) are $\leq 0.3\%$ and $\leq 0.2\%$, respectively, and with respect to all stopping K^- interactions, these rates are $\leq 0.02\%$ and $\leq 0.01\%$.

It is more desirable to express the production rate for (Σ^-n) in terms of a (Σ^-n) singlet production rate since we already know that a triplet (Σ^-n) bound state is unlikely. However, it is not possible to fix the number of productions which could lead to a singlet (Σ^-n) bound state without complicated calculations involving reaction (2b). However, singlet (Σ^-n) production is possible for K^- capture in He^4 as opposed to K^- capture

TABLE II. Σ^- -nucleon bound-state production rates in helium.

Channel	Rate (Σ^-n) (%)	Rate (Σ^-nn) (%)
(2d) $\Sigma^- + \pi^+ + d + n$ $(12 \pm 4.5)\%$ ^a	$\lesssim 3.0$	
(2e) $\Sigma^- + \pi^+ + p + n + n$ $(29 \pm 4)\%$ ^a	$\lesssim 1.0$	$\lesssim 0.7$
Sum of (2d) + (2e) $(41 \pm 3.5)\%$ ^a	$\lesssim 0.7$	
Sum of (2d) + (2e) and $\Sigma^- + \pi^+ + \text{H}^3$ (457) from at-rest K^- 100%	$\lesssim 0.3$	$\lesssim 0.2$
All stopping K^- (8370)	$\lesssim 0.02$	$\lesssim 0.01$

^a The branching rates shown are the fractions relative to the total number of Σ^- hyperons produced (with π^+), that is the sum of reactions (2d) + (2e) + $\Sigma^- + \pi^+ + \text{H}^3$.

¹⁹ For reaction (2d), we estimate by a phase-space calculation that there should be seven more events involving invisible deuterons and for reaction (2e), we similarly estimate that there should be 19 more invisible protons.

²⁰ For all the rate calculations, the errors are statistical only.

¹⁸ Helium Bubble Chamber Group (presented by M. M. Block), in *Proceedings of the Tenth Annual International Conference on High-Energy Physics, Rochester, 1960*, edited by E. C. G. Sudarshan *et al.* (Interscience Publishers, Inc., New York, 1961), p. 426.

in d , since the three-body final state involves many angular momentum partial waves.⁶

It is very significant that all Σ^- are not produced via reaction (2a), the triton channel, since it indicates that there is, in principle, the possibility of producing Σ^- -nucleon bound states. In fact, we have observed 45 examples of reaction (2b) with visible deuterons, $K^- + \text{He}^4 \rightarrow \Sigma^- + \pi^+ + d + n$. The only difference between these events and (Σ^-n) bound state events is that in the first case the Σ^- and neutron are bound and in the second case they are not bound. In addition, in this channel we have searched for a (Σ^-n) final-state interaction. Figure 3 shows the invariant mass of the (Σ^-n) two-body system deduced from these fits. This distribution is not consistent within the limited statistics with curve *A* (Fig. 3), the prediction for a maximally strong final-state interaction between the Σ^- and the neutron. However, the data are consistent with curve *B* which assumes a weaker Σ^- -neutron final-state interaction.²¹

We have found 105 examples of the reaction (2e) with visible protons, $K^- + \text{He}^4 \rightarrow \Sigma^- + \pi^+ + p + n + n$. The presence of $\sim 30\%$ of all Σ^- events in this channel is important in that it again indicates that Σ^- and neutrons are present together in the final state and there is the opportunity for them to form Σ^- -nucleon bound states if the Σ^- -nucleon interaction were strong enough.

Our search for the (Σ^-n) and (Σ^-nn) bound states can be related to the results of hyperon-proton scattering obtained at the University of Heidelberg and the University of Maryland.⁵ From these scattering experiments together with theoretical considerations, it was found that the (Σ^+p) singlet interaction is probably not strong enough to result in a singlet (Σ^-n) bound state. This follows since if the (Σ^+p) singlet interaction was maximal, and the triplet interaction negligible, an

²¹ The conclusion that we do not detect a maximally strong (Σ^-n) final-state interaction, based on our observations of the (Σ^-n) invariant-mass spectrum, depends on the following theoretical calculations which we have performed. These calculations are thought to hold for the case of a strong attractive final-state interaction and assume a final-state-interaction transition amplitude, $T = e^{i\delta} \sin\delta/q$, as discussed by K. M. Watson [Phys. Rev. **88**, 1163 (1952)] and use data from Σ^-p elastic scattering as the source for an estimate of the phase shift δ (via the effective-range expansion); see, in particular, H. G. Dosch and V. F. Muller, Phys. Letters **19**, 320 (1965). The invariant-mass distribution is calculated for various scattering lengths by numerically integrating over four-body phase space with the aid of an IBM 360/40 computer. Assuming all the scattering is in the singlet channel and that the Σ^+p interactions were strong and maximal, we would expect a singlet scattering length of $\sim 5F$. For $a_s = 5F$, the (Σ^-n) invariant-mass spectrum predicted for this final-state interaction, curve *A* of Fig. 3, does not agree with our observations, $P(\chi^2) \simeq 10^{-6}$. On the other hand, if we use a singlet scattering length $a_s = 2 \pm 0.3F$, which corresponds to a measured total Σ^+p cross section of 109 ± 23 mb (Ref. 5), the resulting (Σ^-n) invariant-mass spectrum for this weaker final-state interaction, curve *B* of Fig. 3, agrees with our observations $P(\chi^2) = 0.47$. These studies indicate therefore, that our failure to observe a maximally strong (Σ^-n) final-state interaction in this experiment is consistent with independent results from Σ^+p elastic scattering. In addition, we have calculated the (Σ^-n) invariant-mass spectrum from a pure impulse picture, namely, $K^- + p \rightarrow \Sigma^- + \pi^+$ with $d + n$ as spectators. The (Σ^-n) invariant-mass spectrum predicted does not agree with the data in Fig. 3.

elastic-scattering cross section of $\pi\lambda^2 \simeq 245$ mb would be expected. On the other hand, the elastic-scattering measurements themselves yielded a total (Σ^+p) cross section of 109 ± 23 mb. This indicates that even if all the scattering were in the singlet channel, the (Σ^+p) singlet interaction is much less than maximal. A calculation of Herndon and Tang²² implies that a singlet (Σ^-n) bound state could exist only for a maximal (Σ^+p) singlet interaction. Similar results are expected for the (Σ^-nn) bound state. So the absence of a (Σ^-n) or (Σ^-nn) bound state therefore agrees with conclusions deduced from experiments involving Σ hyperon-proton scattering.

V. CONCLUSIONS

The results of this study can be summarized as follows:

- (1) There were no unambiguous (Σ^-n) and (Σ^-nn) bound-state events observed in this experiment.
- (2) An upper limit on our observation of Σ^- -nucleon bound states corresponds to a rate of $\lesssim 1\%$ of the known Λ hyperfragment production rates in helium.
- (3) There is no maximally strong (Σ^-n) final-state interaction observed within the statistics of this experiment.
- (4) These observations are in agreement with a weak Σ^- -nucleon interaction as deduced from Σ^+ -proton scattering.

ACKNOWLEDGMENTS

We wish to thank Dr. M. Derrick, Dr. T. Fields, Dr. L. Hyman, Dr. J. Fetkovich, and Dr. E. G. Pewitt of Argonne National Laboratory and Carnegie-Mellon University for the film and other assistance. In addition, we are indebted to those who have loaned valuable equipment. The important contributions of Dr. J. H. Boyd, Dr. H. A. Rubin, and J. Glenn McComas are acknowledged. Finally, we appreciate the valuable discussions with Professor George Snow.

APPENDIX

Figure 4 shows the coordinate system used for this impulse calculation. In the model chosen, the K^- is

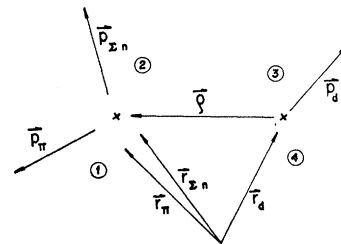


FIG. 4. Coordinate system used for the impulse-model calculation discussed in Appendix. The four nucleons in the initial α particle are represented by 1, 2, 3, and 4.

²² Y. C. Tang and R. C. Herndon, Phys. Rev. **151**, 1116 (1966).

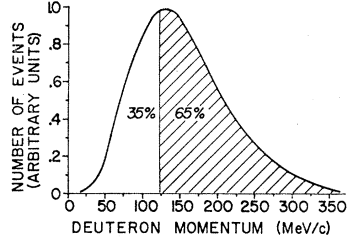


FIG. 5. Deuteron momentum spectrum for the reaction $K^- + d \rightarrow (\Sigma^- n) + \pi^+ + d$ predicted from the impulse model calculation discussed in Appendix. The shaded area is the portion observable in this experiment (mean projected length ≥ 1 mm).

assumed to interact with the center-of-mass of nucleons 1 and 2 changing them into a $(\Sigma^- n)$ and a π^+ with a spectator deuteron. The probability of this taking place with a specified deuteron momentum $R(p_d)d p_d$ equals the sum over all possible final states, with fixed deuteron momentum, of the probabilities of transition to those final states. Lorentz-invariant phase space may then be separated from the transition matrix element squared.

$$R(p_d)d p_d = \int \cdots \int \delta^4(p_\pi + p_{\Sigma, n} + p_d - p_K - p_{He}) \times \prod_{\pi, (\Sigma n), d} \delta(p_i^2 - m_i^2) d^4 p_i |M|^2, \\ M = \int d^3 \tau \langle \text{initial} | S | \text{final} \rangle.$$

The p_i are the 4-momenta of the π^+ , $(\Sigma^- n)$, and d . The initial state may be written as a product of a p -wave K^- Bohr wave function evaluated at the origin^{10,23} and a Hulthén α -particle wave function. The parameters $\mu = 0.8 \text{ F}^{-1}$ and $\nu = 1.25 \text{ F}^{-1}$ were chosen to fit the proton

²³ P. Said and J. Sawicki, Phys. Rev. **139**, B991 (1965), and references therein.

helium scattering data.²³ The final state may be written as a product of outgoing plane waves with an internal distribution function for both the deuteron and the weakly bound $(\Sigma^- n)$ system ($\ll 1 \text{ MeV}$). The wave functions are assumed to be approximately constant over a region the size of an α particle.

$$M = \int d^3 \tau \left\langle \psi_{\text{Bohr}}^p(0) \frac{e^{-\mu \rho} - e^{-\nu \rho}}{\rho} \times |S| e^{i p_\pi \cdot r_\pi} \phi_d e^{i p_d \cdot r_d} \phi_{\Sigma n} e^{i p_{\Sigma n} \cdot r_{\Sigma n}} \right\rangle.$$

Assuming that there are no final-state interactions, we may write $r_\pi = r_{\Sigma n}$ and the c.m. frame $\mathbf{p}_\pi + \mathbf{p}_d + \mathbf{p}_{\Sigma n} = 0$. Furthermore, neglecting any dynamics, such as resonances, S may be taken as a constant.

$$M \propto \int d^3 p \frac{\partial}{\partial p_d} \left(\frac{e^{-\mu \rho} - e^{-\nu \rho}}{\rho} e^{i p_d \cdot \rho} \right), \\ M \propto p_d \left(\frac{1}{(\mu^2 + p_d^2)^2} - \frac{1}{(\nu^2 + p_d^2)^2} \right).$$

This matrix element is a function only of the deuteron momentum, and therefore the phase-space factor may be integrated over all momenta except p_d and multiplied by the matrix element squared, to give the impulse-model prediction for the deuteron-momentum spectrum shown in Fig. 5.

In this experiment we are sensitive to all possible $(\Sigma^- n)$ bound-state events for which the projected deuteron track is greater than 1 mm long. This corresponds to a mean production deuteron momentum of $\sim 122 \text{ MeV}/c$. From Fig. 5 it is seen that this model predicts that we are sensitive to 65% of the expected $(\Sigma^- n)$ bound-state production events.